frontiers | Frontiers in Protistology

TYPE Original Research
PUBLISHED 12 August 2024
DOI 10.3389/frpro.2024.1428985

OPEN ACCESS

EDITED BY
Jean-David Grattepanche,
Temple University, United States

REVIEWED BY
Marija Gligora Udovic,
University of Zagreb, Croatia
Weiwei Liu,
Chinese Academy of Sciences (CAS), China

*CORRESPONDENCE
Thomas Posch
posch@limnol.uzh.ch

RECEIVED 07 May 2024
ACCEPTED 24 July 2024
PUBLISHED 12 August 2024

CITATION
Schalch-Schuler M, Wüest A, Dirren-Pitsch G, Niedermann R, Bassin B, Köster O, Pernthaler J and Posch T (2024) Variability of winter cooling affects intensity of phytoplankton spring blooms – how resilient is the ciliate assemblage composition to changes in food availability? *Front. Protistol.* 2:1428985.
doi: 10.3389/frpro.2024.1428985

Variability of winter cooling affects intensity of phytoplankton spring blooms – how resilient is the ciliate assemblage composition to changes in food availability?

Martina Schalch-Schuler[1], Alfred Wüest[2,3], Gianna Dirren-Pitsch[1], Rafael Niedermann[1], Barbara Bassin[1], Oliver Köster[4], Jakob Pernthaler[1] and Thomas Posch[1]*

[1]Limnological Station, Department of Plant and Microbial Biology, University of Zurich, Kilchberg, Switzerland, [2]Physics of Aquatic Systems Laboratory, Margaretha Kamprad Chair, Institute of Environmental Engineering, École Polytechnique Fédérale de Lausanne, Lausanne, Switzerland, [3]Eawag, Swiss Federal Institute of Aquatic Science and Technology, Surface Waters – Research and Management, Kastanienbaum, Switzerland, [4]Zurich Water Supply, Zurich, Switzerland

After years of partial winter mixing in Lake Zurich (Switzerland), a complete turnover of the water column reoccurred during winter/spring 2021. It was favored by a cold, windy winter and a small difference of water temperatures between the surface zone and a hypolimnion (deep water zone) that had gradually warmed during the previous years. The trend of declining phytoplankton spring blooms due to incomplete winter mixing was interrupted by mass development of algae due to the upwelling of nutrients accumulated in the hypolimnion. The effects of this singular deep mixing on the microbial food web during spring were studied in a high-frequency sampling campaign and compared with data from two years of partial winter mixing (2020 and 2022). A particular focus was put on the quantitative composition of the ciliate assemblage. Our results showed that not all organisms reacted equally to the nutrient (phosphorus) boost in the surface zone. Centric diatoms and cryptophytes profited most directly from the deep mixing, outcompeting the otherwise dominant cyanobacterium *Planktothrix rubescens*. Heterotrophic bacteria and their top predators, the 'heterotrophic nanoflagellates' trophic guild, were less affected by the nutrient supply and showed only short-lived increases of maximal biomass. The assemblage composition of ciliate morphotypes was highly resilient over the three years, presumably due to the range of acceptable food items of the predominant omnivorous species. However, numerous ciliate morphotypes showed brief mass development in 2021, and *Balanion planctonicum*, small *Urotricha* species and tintinnids were significantly more frequent than in 2020/2022. Small interception-feeding morphotypes apparently profited from the rich supply of their cryptomonad food, and tintinnid morphotypes additionally benefited from the availability of building material (e.g., centric diatom shells) for their loricae. In summary, we

show that effects of lake warming in deep stratifying lakes are not as unidirectional as previously presumed, and we reveal resilience of the pelagic ciliate morphotype assemblage to lake warming related interannual variability in Lake Zurich.

KEYWORDS

complete turnover, deep winter mixing, freshwater microbial food web, lake warming, Lake Zurich, pelagic ciliates, phytoplankton spring bloom, resilience of freshwater food webs

1 Introduction

Lakes around the world are affected by warming. Surface water temperatures have risen steadily over the past century in response to increasing air temperature (Woolway et al., 2020; Dokulil et al., 2021) and global radiation (Schmid and Köster, 2016), and lake warming is expected to even aggravate in the future (Råman Vinnå et al., 2021; Desgué-Itier et al., 2023). However, the extent of lake warming varies; it depends on the prevailing local air temperature, wind conditions (O'Reilly et al., 2015) and lake morphology (Toffolon et al., 2014). Lakes in the mid and high latitudes of the northern hemisphere have undergone greater warming than those in low latitudes and the southern hemisphere (Schneider and Hook, 2010). In Central Europe, both warming of surface water in spring and summer (Posch et al., 2012; Yankova et al., 2016) and reduced cooling in winter have been observed (Dokulil, 2014). The resulting discrepancy in heat content between surface and deep water leads to a strengthening of the thermal stratification and water column stability and thus to an earlier onset and prolongation of seasonal stratification (Shimoda et al., 2011; Dokulil, 2014). This development has a negative impact on the intensity and duration of winter mixing in deep lakes (Woolway and Merchant, 2019), which in turn has profound consequences for nutrient-poor (oligotrophic and oligo-mesotrophic) systems: It directly affects the oxygenation of the deep water zone (hypolimnion) (Schwefel et al., 2016) and the upwelling of nutrient-rich deep water into the surface zone (epilimnion) (Salmaso et al., 2018; Schwefel et al., 2019), which is essential for lake productivity (O'Reilly et al., 2003; Yankova et al., 2017).

Lake Zurich, a deep oligo-mesotrophic Swiss lake (Peeters et al., 2002; Knapp et al., 2021) is a representative example for documented changes in thermal stratification and mixing regime due to climate warming. Since the 1970s, surface temperatures in Lake Zurich have increased steadily by 0.39°C per decade as to data collected by Zurich Water Supply (Knapp et al., 2021). The number of winters with shallow mixing (not affecting the deep hypolimnion) has steadily increased since the 2000s (Posch et al., 2012), and since 2013, holomixis (complete water turnover affecting the entire water body) seems to be the exception rather than the rule (Yankova et al., 2017). The resulting decrease in epilimnetic nutrients due to diminished replenishment from the deep hypolimnion has persistently affected phytoplankton blooms in early spring. Based on a long-term dataset (since 1975) of the total phytoplankton community (monthly samples analyzed according to Utermöhl, 1958), it was shown that both, centric diatoms and cryptophytes, are the first and quantitative dominant eukaryotic algae reacting on vernal nutrient replenishment in Lake Zurich. However, low epilimnetic phosphorous concentrations likely have hampered algal growth, especially of centric diatoms, but also of cryptophytes (Yankova et al., 2017). On the other hand, nutrients, especially orthophosphate (PO_4), has accumulated in the deep hypolimnion during periods with incomplete water turnover. In contrast, the cyanobacterium *Planktothrix rubescens* has benefited from prolonged thermal stratification and weak winter mixing, promoting its mass development in summer (Posch et al., 2012; Knapp et al., 2021).

Shifts in phytoplankton abundance and composition determine the occurrence and growth of primary consumers and their predators within aquatic food webs (Sommer et al., 2012). Accordingly, numbers of zooplankton (Phyllopoda and Copepoda) in Lake Zurich have also been declining for decades (Yankova et al., 2017). However, it is not known what effect the altered mixing regime and epilimnetic nutrient availability have on other important grazers of phytoplankton. Ciliates (Ciliophora) form a monophyletic group of morphologically very divers unicellular eukaryotes and are key elements of the planktonic food web. As the first and most effective grazers of phytoplankton, they play a particularly important role during the spring bloom (Posch et al., 2022). Furthermore, ciliate assemblages affect several trophic levels, as they also harbor omnivorous, bacterivorous, and even predatory species (Weisse, 2017). They thus act as central energy pathway by channeling carbon and nutrients from their food source to higher trophic levels, i.e., to their main consumers such as rotifers, cladocerans, and copepods (Sanders and Wickham, 1993).

The most recent climate scenarios predict further warming of Lake Zurich in the coming decades (Råman Vinnå et al., 2021). While the effects of the resulting incomplete winter turnover have already been studied (Yankova et al., 2017), the consequences of a sporadically reoccurring holomixis after a long period of incomplete

winter mixing have not been explored (Holzner et al., 2009). Such a scenario would lead to intense nutrient enrichment of the upper water layer and consequently strongly favor the phytoplankton (Lepori et al., 2018).

During high-frequency spring bloom sampling campaigns in Lake Zurich, effects of a nearly complete turnover was studied as deep mixing reoccurred in winter 2021, within a multi-annual long period of incomplete winter mixing. Here we present in detail three aspects of this nutrient pulse: (i) We analyzed physicochemical parameters to describe the functioning of complete winter mixing and the effects on oxygen and nutrient concentrations in the water column (including a total phosphorus budget of Lake Zurich) during spring. (ii) We quantified the vernal succession of microbial food web components in the seasons after deep winter mixing and compared this dataset with observed dynamics during two years with only partial winter mixing. We analyzed the differences in the quantity of centric diatoms and cryptophytes, bacteria, heterotrophic nanoflagellates (HNF), ciliates and rotifers for three consecutive years, i.e., 2020 (partial mixing), 2021 (deep mixing) and 2022 (partial mixing). (iii) Particular emphasis was put on the composition of the pelagic ciliates assemblage and their role in the food web, i.e., as link between lower (phytoplankton, bacteria, HNF) and higher (rotifers) trophic levels.

2 Material and methods

2.1 Lake Zurich

Lake Zurich is an oligo-mesotrophic, prealpine lake situated in a densely populated, economically important region in the northern part of Switzerland (Bossard et al., 2001). The lake is separated by a natural dam in two major basins: an upper, shallow part (z_{max} = 48 m, 21.7 km^2, 0.4 km^3), fed by the Linth River, and a lower, much deeper part (z_{max} = 136 m, 66.6 km^2, 3.3 km^3), herein referred to as Lake Zurich. This part of the lake is monomictic, with meanwhile irregular holomixis between February and March, typically followed by a summer-long period of thermal stratification.

2.2 Sampling and measurements of *in situ* parameters

Sampling of the Lake Zurich water column was conducted biweekly over four consecutive years (September 2019 until December 2022) at the long-term monitoring site, located close to the deepest point of the lake (47°18'16"N, 8°34'31"E, z_{max} = 136 m). In spring 2020–2022 (February–May), sampling was carried out in shorter intervals: biweekly to weekly in 2020 at the long-term monitoring site and three times per week in 2021 and 2022 in the vicinity of the Limnological Station Kilchberg (47°19'31'' N, 8°33'81'' E, z_{max} = 100 m). During the spring campaigns, samples for the analysis of bacteria, HNF, phytoplankton, ciliates and rotifers were collected from 1 to 8 m depth with an integrating water sampler (IWS 3, Hydro-Bios Apparatebau, Germany). Samples were stored in a 10 L container and brought directly to the laboratory, where they were immediately processed according to the workflow of Figure 1. Physicochemical and biological *in situ* parameters, i.e., water temperature (°C), oxygen concentration (mg O_2 L^{-1}) and *in vivo P. rubescens*-related chlorophyll *a* concentration (µg Chl *a* L^{-1}; Beutler et al., 2002; Hofmann and Peeters, 2013) were measured throughout the entire water column using a multiparameter probe (6600 V2, YSI Incorp., United States) and a TS-16-12 fluoroprobe (bbe Moldaenke GmbH, Germany), respectively. A specific calibration via optical fingerprints for the detection of *P. rubescens* was first described by Leboulanger et al. (2002) and is meanwhile included in the basic setup of the commercially available bbe fluoroprobes. We could show in a long-term (12 years) comparison of both parameters (see Supplementary Figure S2 in Knapp et al., 2021) that *in vivo* related chlorophyll *a* measurement is a good proxy for *P. rubescens* biovolume. The detection of *P. rubescens* via the phycoerythrin-specific sensor of the multiparameter probe proofed as inadequate as this sensor does not differentiate between signals originating from *P. rubescens* and cryptophytes. Profiles of temperature and oxygen were used to determine the mixing depth in early spring. Maximal mixing depth was defined as the depth, where oxygen concentration and temperature abruptly increased (Supplementary Figure 1).

Concentrations of total phosphorus (P_{tot}), PO_4 and silica were measured at 17 distinct depths (0–136 m) monthly throughout the sampling period and additionally biweekly in March and April (0–20 m) by Zurich Water Supply. Seasonal phosphorus inventories were established by volume-integration of the P_{tot} concentration profile, assuming homogeneity within topographically defined horizontal layers. The phosphorus discharge via the Limmat River outflow was calculated using the average P_{tot} content in the uppermost 5 m of Lake Zurich and the water outflow rate from https://www.hydrodaten.admin.ch. Daily values of air temperature were obtained from the Mythenquai Meteorological Station managed by the Zurich Water Police (https://tecson.ch).

2.2.1 Flow cytometric analysis of bacteria

For bacterial counts, 10 mL lake water was fixed with formaldehyde (2% final conc.) and cells were stained with SYBR Green I (Merck Sigma Aldrich, Germany) before bacterial abundances were evaluated in triplicates of 190 µL subsamples via flow cytometry (Cytoflex S, Beckman Coulter, United States). The excitation was set at 488 nm and the emission was measured at 525 ± 20 nm. Bacterial counts included both, heterotrophic bacteria and coccoid cyanobacteria, the latter with an average percentage of 0.13% (maximum 0.52%) on total counts for all years of investigation. Bacteria with high and low nucleic acid content were quantified from cytograms plotting side scatter vs. green fluorescence.

2.2.2 Quantification of selected phytoplankton groups and HNF

Abundances of HNF and selected phytoplankton groups, i.e., cryptophytes (*Cryptomonas* spp., *Rhodomonas* spp.), and centric diatoms (small diatoms: Ø 5–10 µm and large diatoms: Ø 10–25 µm), were determined via fluorescence labelling. Therefore, 40 mL

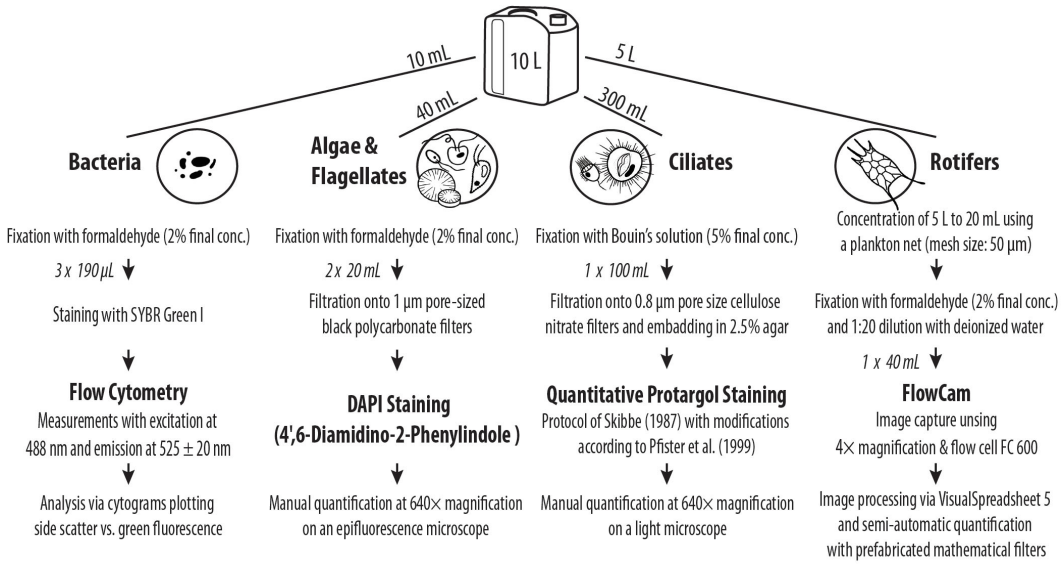

FIGURE 1
Workflow for the quantification of bacteria, phytoplankton (*Cryptomonas* spp., *Rhodomonas* spp. and centric diatoms) and heterotrophic nanoflagellates (HNF), ciliates and rotifers.

lake water was fixed with formaldehyde (2% final conc.), filtered in duplicates (each 20 mL) onto 1 µm pore-sized, black polycarbonate filters (Whatman, Germany) and stained with 4',6-Diamidino-2-Phenylindole (DAPI; Porter and Feig, 1980). Organisms were manually counted at 640× magnification with an Axio Imager M1 epifluorescence microscope (Zeiss, Germany) applying UV-excitation (365 nm) and green-excitation (546 nm) to check for the presence of chlorophyll, respectively. At least 50 counting fields were evaluated per filter, corresponding to an average of 450 (130–2,065) counted cells per sample.

2.2.3 Quantification of ciliates

For the quantification of ciliates, 300 mL of water samples were fixed with Bouin's solution (5% final conc.; containing 10.71 mL picric acid (100%), 3.57 mL formaldehyde (37%) and 720 µL glacial acetic acid (15%); Skibbe, 1994). Subsamples of 100 mL were filtered onto 0.8 µm pore size cellulose nitrate filters (Sartorius, Germany) with counting grids of 9 mm^2 per square and embedded in 2.5% agar (Agar Noble, DifcoTM, Becton Dickinson, United States). Subsequently, Quantitative Protargol Staining was performed following the protocol of Skibbe (1994) with modifications according to Pfister et al. (1999). Finally, the filters were preserved in Canada Balsam (Merck Millipore, Germany). Ciliate abundances were determined at 640× magnification on a Zeiss Axio Imager M1 microscope. At least six squares or a minimum of 250 ciliates per filter were counted. Finally, to record the full diversity of ciliates, the entire filter was re-examined for the presence of rare morphotypes. Morphological identification and description of feeding types was done according to the taxonomy keys by volumes I–IV of Foissner et al. (1991, 1992, 1994, 1995) and Foissner et al. (1999). The classification systems by Gao et al. (2016) and Lynn (2008) were consulted for the taxonomic affiliation of the detected species. Net growth rate was determined for ciliate morphotypes that contributed to the maxima of total ciliate abundance in 2021 (9^{th} April–16^{th} April). For this purpose, exponential growth rates were estimated as $r = ln(N_t/N_0)\ t^{-1}$, where r is the rate of population growth (d^{-1}), N_0 and N_t are the initial and final population densities and t the time since sampling day 0, respectively.

2.2.4 Quantification of rotifers

Five liters of lake water were concentrated to 20 mL using a plankton net with a mesh-size of 50 µm and fixed with formaldehyde (2% final conc.). Quantification and identification of rotifers were performed with an image flow cytometer (FlowCam 8000; Yokogawa Fluid Imaging Technologies, USA), a combination of flow cytometer and light microscope, equipped with a camera. To avoid clogging, the samples were diluted with deionized water in a ratio of 1:20. Of these, subsamples of 40 mL (corresponding to an original volume of 500 mL) were analyzed using 4× magnification and a flow cell FC600. Particles in the range of 15–1,000 µm were captured in the auto-image mode. Image processing and analysis was conducted with the provided software VisualSpreadsheet 5. By gathering around fifty images of each rotifer morphospecies from different perspectives, image libraries were created manually for the most abundant morphospecies: *Asplanchna* spp., *Kellicottia longispina*, *Polyarthra vulgaris*, *Keratella quadrata* and *Keratella cochlearis*. Based on these libraries, mathematical filters were created that allowed the automatic assignment of images to the respective species. The resulting assignments were manually reviewed, and the remaining images were examined for undetected rotifers. The software thus allowed for a semi-automatic quantification of the most common morphotypes.

2.2.5 Carbon content

The cellular carbon content (C-content) was calculated from volumetric measurements or, in the case of rotifers, based on values from the literature (Table 1). The total C-content (biomass) was calculated by multiplying the cellular C-content (organismic carbon in case of rotifers) times the respective total abundances of the organismic entities. Average cell volume of bacteria was determined according to Posch et al. (2009) using size measurements from samples taken in spring 2019 for Lake Zurich. We measured the average cell parameters of DAPI-stained HNF (n=60 cells) and calculated the average cell volume based on geometric formulae. Average cell volume was converted to cellular carbon content via the formula published by Børsheim and Bratbak (1987), using the approach for fixed cells (Table 1). Cell volumes of algal groups were based on live measurements and were provided by Zurich Water Supply. These values were used to determine the cellular C-content (Table 1) of diatoms and cryptophytes separately (Montagnes et al., 1994). Ciliate cell volume was calculated for each species separately, using a geometric formula that most closely resembled the body shape of the species (Supplementary Table 1). A general conversion factor for protists (Table 1) was applied to determine the cellular C-content of each ciliate species (Menden-Deuer and Lessard, 2000).

For inter-annual comparison of the carbon transfer within the microbial food, daily values of biomass were calculated based on interpolation between the sampling days, and finally, the average of all daily values was determined. The same was conducted for *P. rubescens*, using the average concentration of *P. rubescens*-related Chl *a* between 1 and 8 m depths. Results were visualized in a simplified microbial food web according to Fenchel (1987).

TABLE 1 Values of the average body volume (μm^3) of the investigated organismic groups, formulae used to calculate the cellular carbon content (fg C $cell^{-1}$), and the carbon content of one individual in case of rotifers and corresponding references.

	Average body volume (μm^3)	Carbon content (CC) (fg C $individual^{-1}$)	References
Bacteria	V = 0.05 [a]	CC = 218 × $V^{0.85}$	Posch et al., 2009
Heterotrophic nanoflagellates (HNF)	V = 30 [a]	CC = 220 × V	Børsheim and Bratbak, 1987
Algae			
centric diatoms (Ø 5–10 µm)	V = 120 [b]	Diatoms: CC = 287 × $V^{0.811}$ Others: CC = 109 × $V^{0.991}$	Bleiker and Schanz, 1989 Montagnes et al., 1994
centric diatoms (Ø 10–25µm)	V = 2,400 [b]		
Rhodomonas spp.	V = 200		
Cryptomonas spp.	V = 2,100		
Ciliates	individual (based on geometrical shape) [a]	CC = 216 × $V^{0.939}$	Menden-Deuer and Lessard, 2000
Rotifers		Literature value	
Keratella quadrata	V = 0.75 × 10^6	CC = 58 × 10^6	Pauli, 1989
Keratella cochlearis	V = 0.09 × 10^6	CC = 22 × 10^6	Telesh et al., 1998
Kellicottia longispina	V = 0.1 × 10^6	CC = 20 × 10^6	
Polyarthra vulgaris	V = 0.56 × 10^6	CC = 18 × 10^6	
Asplanchna spp. (Ø of >0.5 mm)	V = 51.7 × 10^6	CC = 162 × 10^6	
Asplanchna spp. (Ø of <0.5 mm)	V = 15.3 × 10^6	CC = 63 × 10^6	
Conochilus sp.	V = 0.43 × 10^6	CC = 42 × 10^6	
Brachionus sp.	V = 0.5 × 10^6	CC = 50 × 10^6	

Body volumes are based on own measurements [(a)], obtained from Zurich Water Supply [(b)] or from literature.

2.3 Statistical analysis

Statistical analyses were carried out with the software R (version 4.0.5). Differences between the three years, regarding the vernal biomass of cryptophytes, diatoms, bacteria, HNF, total ciliates and selected ciliate morphospecies, and regarding the chlorophyll content of *P. rubescens* were tested using Mann–Whitney U tests (package stats) followed by a Dunn's tests (package FSA). To differentiate between the high and less productive phase of diatoms and ciliate morphospecies, their biomass dynamics were split into an early (end-February until mid-April) and a late phase before statistical analyses were conducted. False discovery rate of multiple testing was corrected using the Benjamini–Hochberg method.

3 Results

3.1 Physical and chemical parameters

At the beginning of February 2020, temperature differences between surface and deep water were still high (6°C vs. 4.8°C). Due to the still existing density gradient, convective mixing reached only ~80 m depth on February 13th (Supplementary Figure 1). This deep-water replacement caused a temporary increase in oxygen concentration in the hypolimnion and a short upwelling of PO_4 (maximum of 3.5 µg PO_4-P L^{-1}) into the euphotic zone from mid-February to mid-March (Figures 2B, C).

In contrast, in February 2021 two phenomena caused isothermal conditions favoring much deeper mixing: i) unusually high deep-water temperature combined with ii) strong lake surface cooling (Figure 2A). i) In addition to the long-term trend of increasing hypolimnetic temperatures, another substantial warming occurred in spring 2020. As a result, in January 2021, at the end of the stratified period, the temperature at 120 m depth reached 5.2°C (Figure 2A). ii) Low air temperatures, which averaged at 3.1°C (below T_{Lake}) from mid-November 2020 to mid-February 2021, led to a constant strong cooling of the surface water. After one week of average air temperatures of −2°C, the lowest heat content was reached on February 17th, 2021. The cold epilimnetic temperature (~5°C) in combination with the warm hypolimnetic water supported deep convective mixing down to 110 m. Below that depth, the last ten meters above the lake bottom remained stably density-stratified by dissolved solids (Supplementary Figure 1). Deep mixing continued due to relatively long periods of barely

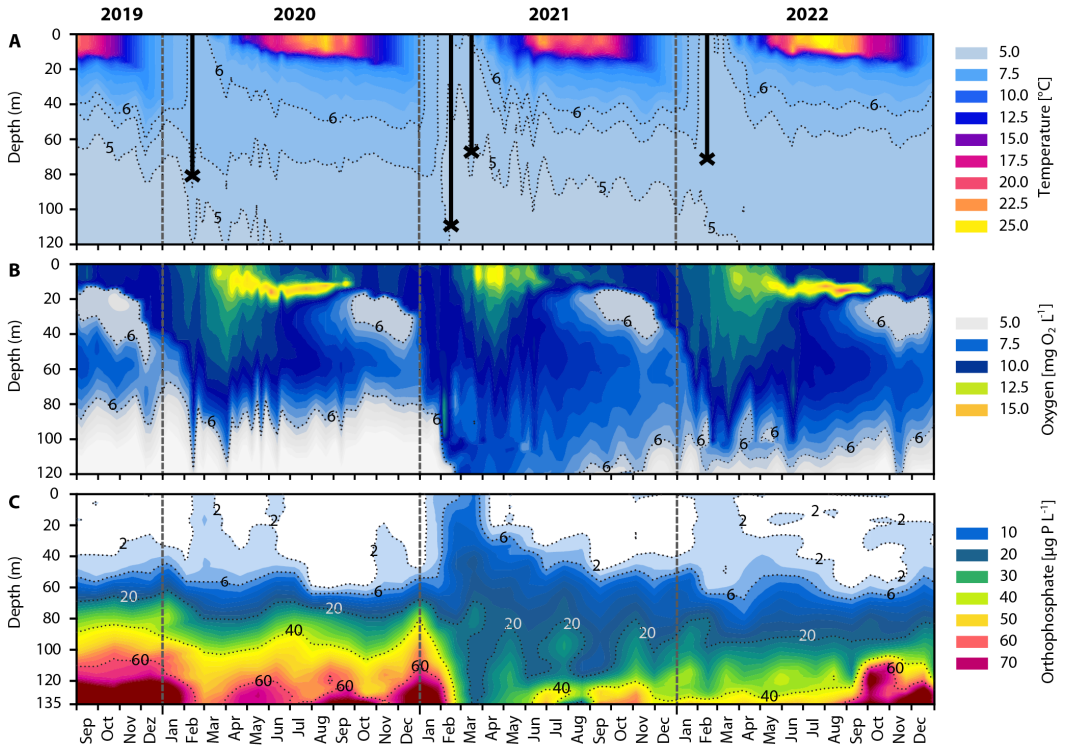

FIGURE 2
Physicochemical parameter contour plot of Lake Zurich from September to December 2019, and for the entire years 2020, 2021 and 2022. **(A)** Water temperature (°C). Black lines with crosses indicate maximal winter mixing depth (see also Supplementary Figure 1). **(B)** Oxygen concentration (mg O_2 L^{-1}). Black dotted line displays the 6 mg O_2 L^{-1} threshold. **(C)** Orthophosphate (PO_4) concentration (µg PO_4-P L^{-1}). Black dotted lines and corresponding values indicate distinct PO_4 isolines. Temperature and oxygen profiles **(A, B)** were measured between 0 and 100/120 m, PO_4 concentration **(C)** between 0 and 136 m. Grey dashed vertical lines represent the beginning of the year.

present warming until late March. During this time, conditions in the lake were characterized by short stratification episodes interrupted by short cooling and shallow mixing events. This led to a continuous homogenization of the water column that resulted in a second unusual deep mixing to ~60 m depth on March 17th (Figure 2A). Deep convective mixing together with recurring turbulences increased the downwelling of oxygen-rich surface water, leading to hypolimnetic oxygen replenishment (Figure 2B). During this period, oxygen concentration at great depth exceeded the 6 mg O_2 L^{-1} threshold, which can be used as a rough proxy for mixing depth (Örn et al., 1981). Hypolimnetic oxygen concentrations remained high until the end of summer 2021. Simultaneously, PO_4 was transported multiple times to the euphotic zone, causing finally a three-fold rise in concentration compared to 2020 (maximum of 8.5 µg PO_4-P L^{-1} in mid-March 2021). A drastic decline in hypolimnetic PO_4 concentrations was observed during that time, which remained at low level until September 2022. In addition, P_{tot} content (including PO_4 as well as particulate and organismic bound phosphorus) of Lake Zurich decreased continuously during the entire year 2021. At the end of 2021 and throughout 2022, P_{tot} was 20 metric tons P lower compared to 2020 (Supplementary Figure 2). Heavy rain falls lasting from May to July in 2021 (MeteoSwiss, 2021) led to a high outflow of the River Limmat and thus to an increase in P_{tot} discharge to 37 tons P $year^{-1}$. In comparison, the calculated annual P_{tot} discharge was only 33 tons P $year^{-1}$ in 2020 and 23 tons P $year^{-1}$ in 2022 (Supplementary Figure 3).

The deep and intense water turnover in 2021 again led to a cooling of the deep water layers (below 5°C, Figure 2A). Together with the relatively warm lake surface at the end of the stratification period in 2021, temperature conditions in 2022 were similar to those in winter 2020. Thus, a partial water turnover to a depth of ~70 m was observed in mid-February 2022 (Supplementary Figure 1) and PO_4 concentrations in the euphotic epilimnion increased only to ~2.7 µg PO_4-P L^{-1}.

3.2 Successions during the spring phytoplankton bloom

An exceptional increase of maximal cell numbers and biomass was observed for nearly all studied organisms (Figure 3A; Supplementary Figure 4). In particular, centric diatoms (mainly *Cyclotella* spp. and *Stephanodiscus* spp.) increased in abundance and thus in biomass already in early spring during the turbulent phase and after the second deep mixing in mid-March. The numbers of large centric diatoms rose to a greater extent than that of small ones, exceeding the maximal biomass of the 2020 population by a factor of six. In 2022, the numbers of centric diatoms remained extremely low throughout the spring period.

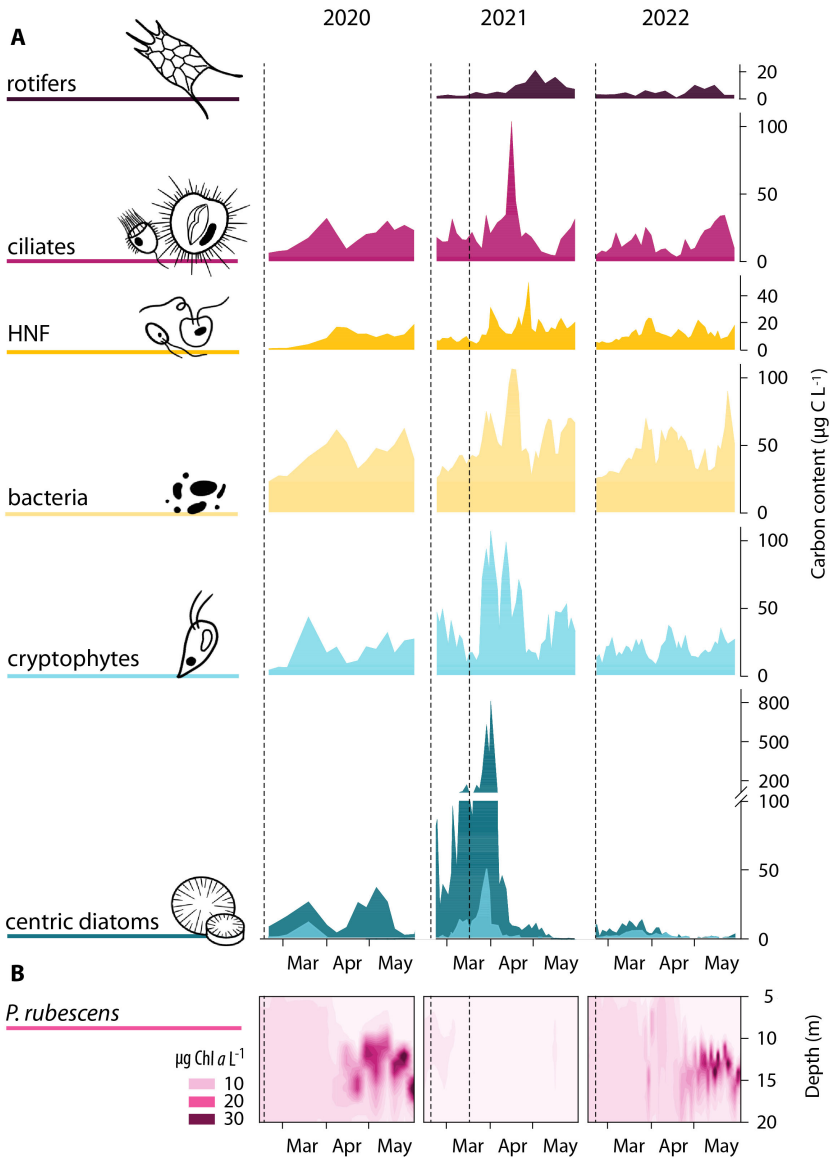

FIGURE 3
Succession patterns of the investigated organisms in Lake Zurich from mid-February to end-May 2020 (left), 2021 (middle) and 2022 (right). **(A)** Biomass (carbon content in µg C L^{-1}) calculated from cell counts and cellular/individual carbon content (Table 1) of rotifers, ciliates, heterotrophic nanoflagellates (HNF), bacteria, cryptophytes and centric diatoms found at a depth between 1 and 8 m. Different size of centric diatoms is indicated by colors, light blue: Ø 5–10 µm, dark blue: Ø 10–25 µm. Biomass of rotifers was analyzed in 2021 and 2022 only. **(B)** *P. rubescens*-related Chl *a* values from 5 to 20 m depth. Dashed lines in **(A, B)** represent times of deep mixing.

Also, biomass of cryptophytes (*Cryptomonas* and *Rhodomonas* spp.) increased by fivefold within one week in April 2021, clearly exceeding the peaks of the years 2020 and 2022 (Figure 3A). In general, peak values of cryptophytes and diatoms were followed by maximum abundances and biomass of bacteria, HNF and ciliates (Figure 3A; Supplementary Figure 4). Towards the end of April 2021, the maxima of these microorganisms were at least twice as high as in 2020 and 2022. Additionally, the proportion of active bacteria (with high nucleic acid content) was also higher in 2021 compared to values observed in the other years (Supplementary Figure 4).

The numbers and biomass of rotifers were analyzed in 2021 and 2022. In both years, rotifer biomass increased towards the second half of spring, with highest values recorded in late April and May (Figure 3A; Supplementary Figure 4). Maximum biomass in 2021, dominated by the species *Keratella quadrata*, *Asplanchna* spp., *Kellicotia longispina* and *Brachionus* sp., exceeded that of 2022 by a factor of two, in the case of *Keratella cochlearis* and *Polyarthra vulgaris* by a factor of five.

Although, after winter, the cyanobacterium *P. rubescens* started with low population densities in all three years, its development during spring varied greatly (Figure 3B). *P. rubescens*-derived Chl *a* in the metalimnion increased towards end-April in the years 2020/22. In contrast, no growth was observed in spring 2021, and the cyanobacterium remained nearly absent for the rest of the stratified season.

3.3 Ciliate succession

In spring 2020, 2021 and 2022, a total of 47 different ciliate morphotypes were identified, 28 at species and 19 at genus level. Of these, 39 morphotypes were observed in all three years (Figure 4A). The proportion of functional groups, i.e., algivorous, bacterivorous, mixotrophic, omnivorous and raptorial ciliates, was similar in all years (Figure 4B). The share of mixotrophs was slightly lower in 2021, compared to the adjacent years, while algivores were more represented in 2021/2022.

Overall, 2021 was an exceptional year regarding ciliate dynamics. Numerous ciliate species had distinctly higher maximal abundances, contributing to peak densities of ~140,000 ciliates L^{-1} on 16th April 2021 (max. 2020: ~33,000 cells L^{-1}; 2022: ~23,000 cells L^{-1}; see also Supplementary Table 2 for maxima of selected ciliate morphotypes). This corresponded to 104 µg C L^{-1}, about three times higher than the maxima in 2020/22 (Figure 3A). This short-lasting peak was dominated by the small algivorous *Balanion planctonicum* (20.3 µg C L^{-1}) and the large mixotrophic *Stokesia vernalis* (29.5 µg C L^{-1}, Figures 4C, D). *B. planctonicum* was also the most abundant morphospecies (75,000 cells L^{-1}) with respect to total ciliate counts, while *S. vernalis* was represented by very low cell numbers (634 cells L^{-1}). Further, tintinnids (*Tintinnidium pusillum* and *Tintinnopsis cylindrata*) were highly abundant in spring 2021 (Figure 4C). Contrary to 2020/2022, maximum values were not observed in early spring but tintinnids further increased until 16th April, resulting in a fourfold higher amount of total biomass (total from mid-February to end-May). Simultaneously, other ciliates like the algivorous small *Rimostrombidium* spp. (mainly *R. hyalinum* and *R. branchykinetum*), omnivorous *Urotricha* spp. (Ø <25 µm), the bacterivorous *Halteria grandinella* as well as raptorial *Askenasia* spp. reached highest abundances and biomass (Figures 4C, D). At this time *B. planctonicum*, *Rimostrombidium* spp. and *Askenasia* spp. reached high net growth rates of 0.5 d^{-1}, followed by tintinnids, *Urotricha* spp. (Ø <25 µm), *Halteria grandinella* with net growth rates of 0.3 d^{-1}. The bacterivorous ciliate *Cyclidium glaucoma* showed similar growth dynamics in all three years, with

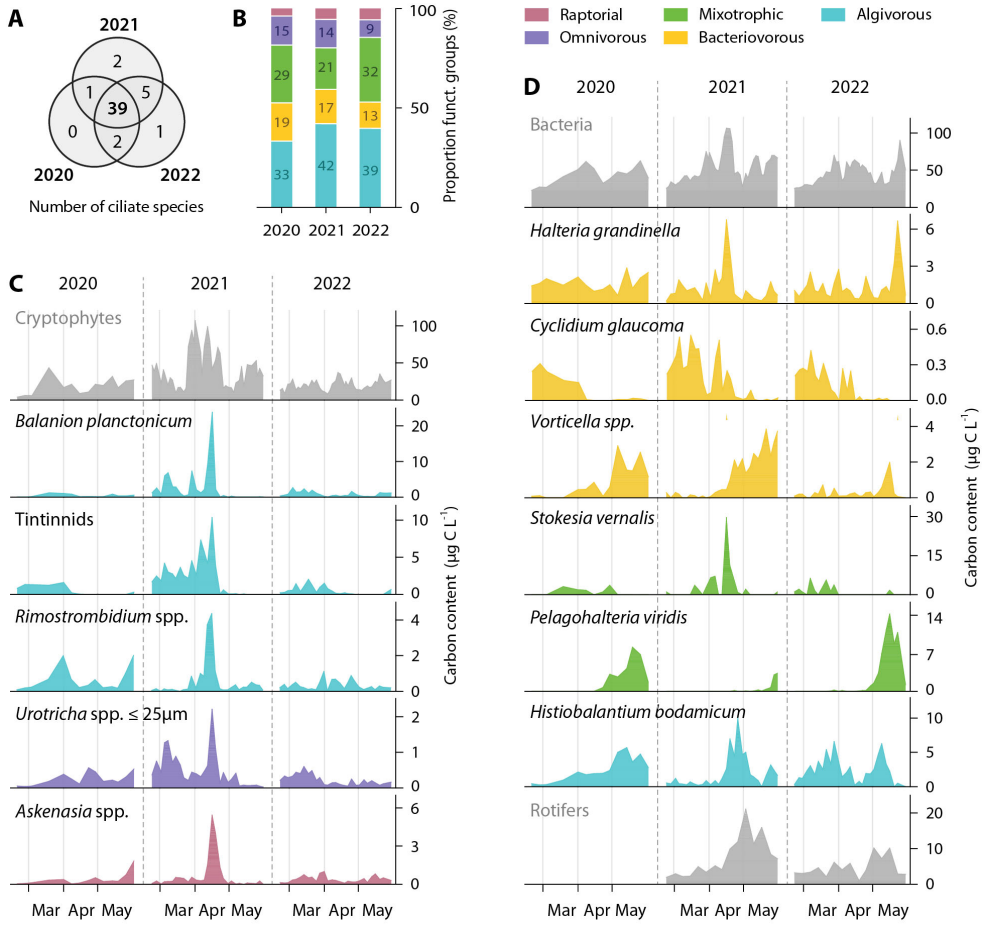

FIGURE 4
Number of ciliate morphotypes **(A)**, their proportion to functional groups **(B)** and succession patterns **(C, D)** from a depth of 1–8 m in Lake Zurich from mid-February to end-May 2020, 2021 and 2022. **(C, D)** Succession patterns showing the biomass (carbon content in µg C L^{-1}) of 11 selected, abundant ciliate morphotypes (see color code at top-right) in combination with potential food sources (cryptophytes and bacteria) and predators/competitors (rotifers), all depicted in grey. Note the different scales for biomass among the different morphotypes/organismic groups. Light-grey lines indicate beginning of the months, grey dashed lines separate the three years. Different colors in **(B–D)** reflect distinct functional groups, shown at the top-right of the figure.

decreasing biomass towards mid-spring (Figure 4D). Again, biomass peaks in 2021 were slightly higher.

After the short-lasting peak in mid-April, the ciliate population declined. Total ciliate biomass decreased to a minimum of ~45 µg C L^{-1} on 17th May 2021 (Figure 3A). Many ciliate morphotypes remained at very low abundances thereafter until the end of the sampling campaign at the end of May. One exception was the large, mainly algivorous ciliate *Histiobalantium bodamicum* (Figure 4D). At the beginning of spring 2021, its biomass was lower than in 2020 and 2022. In late April and early May, however, peak values were 1.5 times higher than those of the other two years. In the second half of spring 2021, also peritrichs of the genus *Vorticella* increased in abundance, exceeding the total biomass of the neighboring years (Figure 4D). In the following year, the *Vorticella* populations decreased drastically and reached only one third of the maximum of 2021. During the study period, the mixotrophic *Pelagohalteria viridis* was the latest representative in the ciliate succession to reach maximum biomass (Figure 4D). In 2021, with a delay of three weeks compared to 2020 and 2022, the peak was even further behind.

3.4 Consequences for the microbial food web

In all three years, the vernal PO_4 enrichment in the epilimnion promoted a bloom of centric diatoms and cryptophytes, which served as nutritional basis for many consumers within the microbial food web. In addition to single high abundance peaks in 2021, also averaged population densities and biomass of the studied autotrophic organisms differed significantly between 2021 and 2020/2022 (Dunn's test, $p<0.05$). Significant differences between the three years were found for diatoms until mid of April, for cryptophytes during the entire spring period. In 2021, total biomass of diatoms increased by fourfold and doubled for cryptophytes relative to the previous year. In contrast, the population density of *P. rubescens* dropped significantly, with 75% less total Chl *a* than in 2020/22 (Figure 5). The effects of phosphorus availability in 2021 on the heterotrophic components of the microbial food web were less pronounced than on phototrophs and no significant difference in biomass was observed for bacteria, HNF and total ciliates during spring (Dunn's test, $p>0.05$). However, biomass of three ciliate morphotypes (*Balanion planctonicum*, *Urotricha* spp. <25µm and tintinnids) increased significantly (Dunn's test, $p<0.05$) in the first half of spring 2021 compared to 2020/2022, whereas other morphotypes showed only short-term maxima in otherwise similar trends to 2020/2022 (Supplementary Table 3). In the second half of spring 2021, the biomass of the mixotrophic species *Pelagohalteria viridis* was significantly lower than in the two other years.

4 Discussion

4.1 Functioning of deep water turnover

While convective seasonal mixing occurred in all three winters, the deeper mixing in 2021 caused a three-fold higher concentration of epilimnetic PO_4 compared to 2020/2022. In February 2021, convective mixing to 110 m depth was favored by isothermal conditions over the water column due to strong surface cooling in combination with relatively warm water at great depth. In contrast, temperature differences between the surface and the hypolimnetic water were too high to support deep winter mixing in February 2020 and 2022. As an effect, the hypolimnetic water temperatures were unusually high at the end of the subsequent stratified period. Besides a long-term trend of increasing temperatures at depth (Knapp et al., 2021), another pronounced warming occurred already in spring 2020. The stepwise warming was most probably induced by lateral inflow of warmer water from the shallow eastern lake domain. Cold nights in January 2020 caused a cooling of these shallow waters to ~5.2°C (alplakes.eawag.ch). Subsequently, these heavier water masses, which were cooler than the central surface but warmer than the deepest waters, flowed westwards to greater depths (Doda et al., 2022; Doda et al, 2023), where these intrusions finally led to warming of the deepest reaches, which remained weakly stratified.

4.2 Loss of total phosphorus through washout

Despite similar winter mixing conditions and phytoplankton bloom dynamics, the P_{tot} content of the pelagic zone and hypolimnetic PO_4 concentrations were lower in 2022 than in 2020 (Supplementary Figure 2). A reason for this discrepancy can be found in the physico-chemical processes observed in the previous year. Deep mixing in combination with recurring turbulences in 2021 did not only result in a striking rise of epilimnetic PO_4 concentrations, but also in a removal of hypolimnetic PO_4. In addition, the high oxygen concentration in the deep zone (Figure 2B) potentially resulted in reduced PO_4 release from the sediment surface (Einsele, 1936; Mortimer, 1942). However, this is not sufficient to explain the overall decrease in P_{tot} in the pelagic zone over the year 2021 (Supplementary Figure 2). An additional important reason might be the persistent heavy rainfalls lasting from May to July in 2021 (MeteoSwiss, 2021). To prevent flooding of the lakeshore, the outflow rate at the Limmat River weir was increased, especially during July (Supplementary Figure 3; https://www.hydrodaten.admin.ch). The higher discharge led to washout of PO_4 and phytoplankton from Lake Zurich, resulting in an overall decrease in P_{tot}. Another reason could be the sedimentation of part of the algal biomass, especially diatoms (Smetacek, 1985), thereby transporting the bound phosphate to the sediment surface, where it was not yet released. In addition, the high P_{tot} export from the productive surface layer in 2021 explains why O_2 consumption by decomposers was not enhanced even though production was highest in this year. This resulted in a persistent high oxygen concentration of the hypolimnion throughout 2021.

4.3 Consequences for the microbial food web

The vernal phytoplankton spring bloom is a recurring phenomenon in Lake Zurich. However, its intensity varies over

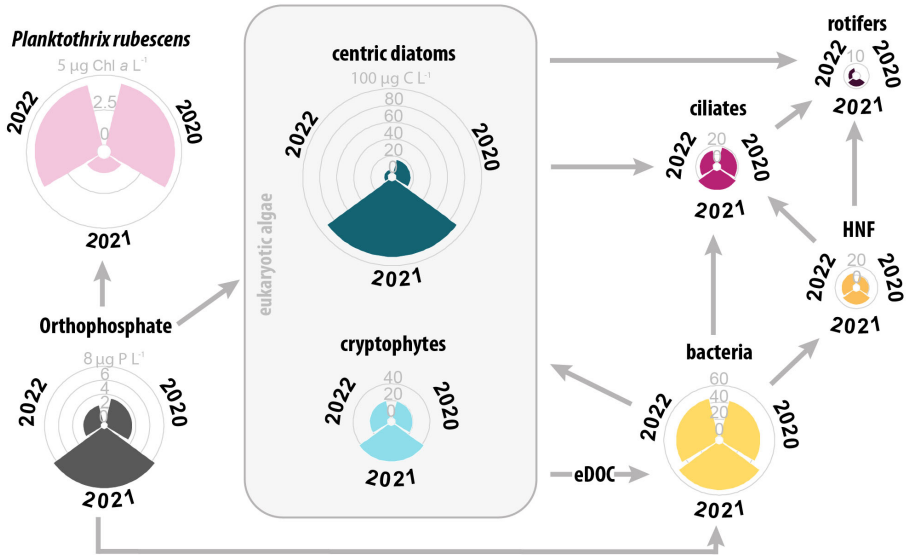

FIGURE 5
Schematic illustration of estimated energy transfer pathways in a simplified microbial food web of Lake Zurich during springtime. Comparison of initial epilimnetic orthophosphate concentration (PO_4-P, in µg P L^{-1}) after winter mixing (average from 1 to 8 m), average daily biomass (µg C L^{-1}) and average Chl *a* value (*P. rubescens*, in µg Chl *a* L^{-1}) during spring (end-February until end-May) of the years 2020, 2021 and 2022. Therefore, arrows represent possible energy fluxes within the food web according to the scheme published by Fenchel (1987).

the years and is influenced by mixing depth and subsequent upwelling of nutrients from the autochthonous pool in the hypolimnion (Yankova et al., 2017). In sum, the maximal abundances of the observed groups in 2021 were exceptional, even compared to dynamics observed during the last 15 years (Table 2). Although similarly high PO_4 pulses have been observed before (2006, 2009, 2012 and 2018), the turbulent mixing episode in March 2021 caused a long-lasting nutrient enrichment of the epilimnion and a striking decline in *P. rubescens* (a major competitor for eukaryotic algae, see below).

4.3.1 Specific phytoplankton groups as profiteers

We focused on two algal groups (centric diatoms and cryptophytes) known to respond faster to nutrient replenishment in spring than other members of the phytoplankton community (Yankova et al., 2017). Additionally, owing to their unambiguous morphologies, both groups could be readily quantified by epifluorescence microscopy. This allowed for a relatively quick evaluation of many samples. However, we are aware that our approach cannot replace the classic quantification of algae by the Utermöhl technique (Utermöhl, 1958) if the entire phytoplankton community is to be analyzed.

Since the restoration of Lake Zurich starting in the 1960s, P_{tot} level have declined, whereas epilimnetic nitrogen concentrations have remained high (Posch et al., 2012). In the early 2000s, phosphorus became the limiting growth factor of phytoplankton in spring owing to reoccurring shallow winter mixing and the resulting insufficient replenishment of nutrients in the epilimnetic zone (Yankova et al., 2017). Despite rising phosphorus availability in 2021, not all studied autotrophic organisms have benefited equally, and centric diatoms were the primary profiteers (Figures 3, 5). These small-sized algae can have even higher growth rates than flagellated algae in the same size range (e.g., cryptophytes) under non-limiting conditions (Reynolds, 2006). Besides phosphorus, the growth of diatoms depends on the availability of silica, an essential component of frustules. However, while epilimnetic PO_4 nearly disappeared in times of partial turnover during the early 2000s, silica slightly accumulated in the euphotic water layer due to reduced consumption (Yankova et al., 2017) and never fell below the critical threshold for diatom proliferation (Supplementary Figure 5; Egge and Aksnes, 1992). Furthermore, along with the favorable nutrient conditions, centric diatoms profited from the turbulent mixing episode in March 2021, allowing them to remain suspended in the euphotic zone for a longer period of time (Huisman et al., 2004). The second profiteers were cryptophytes. These typical r-strategists exhibited high growth rates at end of March, probably as response to high epilimnetic P levels. However, later abundance peaks in April and May hint at a different nutritional strategy less dependent on high P values (Sommer et al., 1986): Some genera of cryptophytes can acquire essential nutrients via mixotrophy by feeding on bacteria (Urabe et al., 2000; Yoo et al., 2017).

4.3.2 *Planktothrix rubescens* and mixing dynamics

Among autotrophic organisms, it was mainly *P. rubescens* (Figures 3, 5) that did not profit from environmental conditions in spring 2021. This filamentous cyanobacterium is usually the dominant phototrophic organism in Lake Zurich and develops massive annual blooms since the 1970s (Posch et al., 2012). Owing to its high toxicity to most eukaryotes (Blom et al., 2003; Kurmayer et al., 2016), predation on *P. rubescens* is very low and it is thought to be a sink rather than a link for nutrients within the food web. The physical downwelling of the filaments below 100 m

TABLE 2 Reported maximal abundances (cells mL^{-1}) of the investigated organismic groups during spring period of the last 10 to 50 years from Lake Zurich.

Year	PO_4 (µg P L^{-1})	Maximal abundances during spring (cells mL^{-1})					
		centric diatoms	cryptophytes	bacteria	HNF	ciliates	reference
2022	2.7	450	1.5×10^3	5.3×10^6	3.6×10^3	23	
2021	**8.5**	**7.3×10^3**	**3.8×10^3**	**6.2×10^6**	**7.6×10^3**	**140**	
2020	3.5	950	1.1×10^3	3.7×10^6	2.6×10^3	32.5	
2019	2.8	300	1.2×10^3	4×10^6	5×10^3	32	11
2018	11.6	5.8×10^3	800	3.2×10^6	–	–	8, 9
2014–2016	1.6–2.5	200–320	500–700	3.5×10^6	6×10^3	25–40	1, 8, 10
2012	11.3	1.2×10^3	1.7×10^3	3.8×10^6	–	–	8, 9
2011	3.7	900	1.5×10^3	4×10^6	8.2×10^3	–	3, 8
2009	10.3	1,000	14×10^3	3.5×10^6	6.5×10^3	60	2,4
2006	9.3	2.5×10^3	950	4×10^6	–	–	5, 8
1983	57.5	~1,000	~2.5×10^3	–	–	–	6[a]
1981	64.2	~13×10^3	~2.7×10^3	–	–	–	7[a]

1) Pitsch et al. (2019); data from 5 m depth.
2) Posch et al. (2015); data from 5 m depth.
3) Eckert et al. (2013); data between 3.5 and 8 m depth.
4) Eckert et al. (2012); data between 3.5 and 8 m depth.
5) Zeder et al. (2009); data from 2.5 m depth.
6) Bleiker and Schanz (1989); integrated from 0 to 20 m depth.
7) Schanz (1986); integrated from 0 to 20 m depth.
8) Unpubl. data: algal abundance from 5 m depth determined by Zurich Water Supply.
9) Unpubl. data: bacterial abundance from 5 m depth determined by the Limnological Station.
10) Master thesis: Pitsch (2015); data from 5 m depth.
11) Master thesis: Schuler (2020); data from 5 m depth.
[a]Data for *Stephanodiscus hantzschii* and *Rhodomonas* spp.
The maxima for our three years of investigation are highlighted in gray. Where necessary, biovolumes were converted to abundance values according to Bleiker and Schanz (1989). Average orthophosphate concentrations after winter mixing between 0 and 20 m depth were determined by the Water Supply Zurich.
Values in bold highlight the high values in the exceptional year 2021.

depth is a limiting factor for *P. rubescens*. High hydrostatic pressure causes the collapse of their gas vesicles needed for buoyancy, thereby trapping filaments in the deep dark zone during winter mixing (Walsby et al., 1998). This was also the case in winter 2021, where deep convective turnover to ~110 m significantly reduced its population size. However, *P. rubescens* is not only influenced by downwelling of filaments, but also by its successful reestablishment in the metalimnion after spring. This is tightly associated with the vertical positioning of filaments in the water column, as triggered by irradiance (Knapp et al., 2021). From mid-February until end-March 2021, short stratification episodes were repeatedly interrupted by shallow mixing events, likely preventing the formation of a stable water column and thus the regrowth of the cyanobacterium during the nutrient-rich period. The absence of *P. rubescens* thus resulted in a competitive advantage for eukaryotic phytoplankton by reducing the dominant nutrient competitor.

4.3.3 Short lasting maxima of bacteria and HNF

The bacterial abundance peak in 2021 exceeded the observed maxima of the last 15 years by a factor of 1.5 (Table 2). Their growth was probably promoted by increased phosphorus availability (Mindl et al., 2005), as well as by the excretions of extracellular dissolved organic carbon (eDOC) from algae (Esteban and Fenchel, 2020). Nevertheless, total bacterial biomass differed marginally between the three years of our investigation (Dunn's test, $p>0.05$; Figure 5) which could be linked to an increased predation pressure regulating the size of the bacterial standing stock. Microcosm experiments showed a similar weak response in bacterial abundance after nutrient addition (Yankova et al., 2017), where phosphorus (20 µg P L^{-1}) was added to epilimnetic water, notable even three times higher concentrations than observed during deep mixing 2021. However, the slightly higher proportion of bacteria with high nucleic acid content in 2021 points to an increased bacterial activity compared to dynamics observed in the neighboring years (Supplementary Figure 4). Bacterial carbon maxima were followed by heterotrophic nanoflagellates as main predators of bacterial biomass. Like bacteria, they had only a temporary higher maximum in otherwise similar trends to 2020/2022 and thus no significant difference between years was observed (Dunn's test, $p>0.05$; Figure 5).

4.4 Consequences for ciliates

By using the classical QPS approach to quantify ciliate morphotypes, we obtained reliable abundance and biomass

estimates of the ciliate assemblage, as well as a data set that could be readily compared with previous studies (Table 2). Earlier attempts to apply next generation sequencing for the quantification of ciliates in Lake Zurich (Pitsch et al., 2019) further confirmed the known problems in ciliate abundance determination by this approach (Santoferrara et al., 2014). Alternatively, fluorescence *in situ* hybridization represents a powerful potential tool for reliably quantifying planktonic ciliate genotypes, as recently demonstrated for Lake Zurich (Dirren-Pitsch et al., 2022). However, the currently available repertoire of specific oligonucleotide probes is still too limited for analyzing the entire ciliate assemblage as presented in this study.

Although environmental conditions differed remarkably between the three years, there was clear resilience in ciliate morphotype composition (Figures 4A, B). The co-occurrence of a wide range of ciliate morphotypes may be due to their highly diversified ecological niches and foraging strategy: numerous ciliate species do not feed exclusively on one type of prey but are rather omnivorous (Posch et al., 2022). However, this study reports the highest ciliate numbers ever observed in Lake Zurich (Table 2).

4.4.1 Ciliates profiting from increasing food sources

Planktonic ciliates have fast doubling rates of <1 to 2 d^{-1}, allowing for immediate response to rising prey availability (Macek et al., 1996). In Lake Zurich, particularly small fast-growing r-strategists benefited from increasing food amounts, including *B. planctonicum* and small *Urotricha* species which reached significantly higher numbers in early spring 2021 than in 2020/2022 (Dunn's test, $p<0.05$).

In spring, *B. planctonicum* is a highly efficient grazer of small algae with preferences for cryptophytes (Tirok and Gaedke, 2007; Posch et al., 2015). It can have high growth rates resulting in up to 2 doublings d^{-1} at 18°C and 1 doubling d^{-1} at 9°C, respectively (Müller and Geller, 1993). These values are slightly higher than our observed net growth rate of 0.5 d^{-1} at ~7°C (1 doubling per 31 h) during the ciliate peak in 2021. There is a niche separation with equally sized, small *Urotricha* species, which feed on similar sized food items but are omnivores that also accept other prey types (Weisse et al., 2001). Small sized *Urotricha* species (e.g., *U. furcata*) are also characterized as r-strategists with slightly lower growth rates than *B. planctonicum* at low to moderate temperatures (5–18°C, Müller and Geller, 1993). Similar observations were made in Lake Zurich, where their net growth rate (0.3 d^{-1}) was below that of *B. planctonicum*, which may explain the observed differences in maximal cell numbers. In our study, small-sized species of the genus *Rimostrombidium* (e.g., *R. humile* and *brachykinetum*) also responded quickly to the phytoplankton bloom with equal growth rates as *B. planctonicum*, and thus represented other efficient r-strategists within the ciliate assemblage. These species prefer small algae with a strong positive selection for cryptophytes (Posch et al., 2015), but can also ingest small centric diatoms (Müller and Schlegel, 1999). However, they were not as abundant as the two morphotypes mentioned above, and no significant differences between the three years could be observed for small *Rimostrombidium* species.

Despite the high biomass of centric diatoms in spring 2021, only a small number of ciliates profited from the rich food supply, because most ciliates cannot grow on an exclusive diet of diatoms (Skogstad et al., 1987). Ciliated interception feeders (e.g., *B. planctonicum*) select against immotile diatoms as a food source, whereas some filter feeders (e.g., *Rimostrombidium* and tintinnids) do not (Müller and Schlegel, 1999). In Lake Zurich, numbers of tintinnids increased significantly in early spring 2021. They benefitted from the high food availability, but also from diatom frustules as construction material for their loricae (Agatha et al., 2012). Remarkably, tintinnids built their loricae exclusively from centric diatom frustules after the large diatom bloom in 2021, whereas it consisted of various detrital particles in other years (Supplementary Figure 6).

Not all r-strategists increased to a similar extent. The fast-growing (up to 2.4 doublings d^{-1}) *Cyclidium glaucoma* was just slightly more abundant in 2021 compared to the neighboring years. The strictly bacterivorous species has moderate ingestion rates in comparison to other bacterivorous ciliate species like *H. grandinella* (Šimek et al., 2019), potentially resulting in exploitation competition between the two species. In addition, abundance peaks of *C. glaucoma* and HNF were temporally shifted, suggesting that *C. glaucoma* was also in competition with flagellates for bacterial prey.

4.4.2 Top-down effects and consequences for the ciliate assemblage

With the proliferation of rotifers and prior to the peak of cladocerans, most ciliates species dropped in abundance towards the end of the investigation period, particularly in 2021. Ciliates are, besides phytoplankton and fine organic aggregates, within the accepted food size range of many planktonic rotifers. Species within the genera *Asplanchna* and *Keratella* were highly abundant in late spring 2021 and are known to prey efficiently on ciliates (Weisse and Frahm, 2002; Gilbert, 2022). Beside predation, food niches of planktonic rotifers overlap with many ciliates leading to an exploitative competition between the two groups (Gilbert, 2022).

However, a few ciliate species, like *Histiobalantium bodamicum*, seemed to benefit from the decline of total ciliate numbers and the concomitantly reduced competition. This large slow-growing species is an inferior competitor to ciliated r-strategists (Müller and Schlegel, 1999), and was significantly less abundant in the first half of spring 2021 than in the second half. In contrast to many other ciliates, it has a jumping like flight behavior similar to the jumping swim style of *Halteria* (Gilbert, 1994), allowing it to escape from rotifer predation.

Peritrichous ciliates of the genus *Vorticella*, mainly as epiphytes on the colonial diatom *Fragilaria*, also increased in abundance at the end of the spring periods 2020 and 2021. On the one hand, attachment is as grazing protection strategy against larger predators, as colonial pennate diatoms are outside the prey size range of most rotifers (Sonntag et al., 2006). On the other hand, sessile peritrichs can generate filtration currents and thus reach higher ingestion rates than their freely swimming competitors (Fenchel, 1987; Esteban and Fenchel, 2020), with grazing rates of up to 8,000 bacteria $ciliate^{-1}$ h^{-1} (Šimek et al., 2019).

4.4.3 Delayed clear water phase

The renewed increase in phytoplankton productivity in the second half of April 2021 resulted in a delayed onset of the clear water phase (period with highest water transparency). The clear water phase goes hand in hand with low primary production and a decline in bacterial and HNF abundance. In this time of low food supply, mixotrophic ciliates benefit from their dual nutrition strategy, i.e., by feeding on particles and by using algal endosymbionts at the same time (Posch et al., 2022). The mixotrophic ciliate *Pelagohalteria viridis* typically becomes abundant at the onset of this period in Lake Zurich (Posch et al., 2015). Due to the delayed onset of the clear water phase in 2021, *P. viridis* occurred two weeks later than in the two other years of investigation, reflecting the significant discrepancy between the years (Dunn's test). By contrast, other mixotrophic ciliates, e.g., *Stokesia vernalis*, already increased during early spring in parallel with r-strategists. This large slowly growing ciliate consumes a wide size range of food particles in addition to harboring endosymbiotic algae and thus probably benefitted from increased prey availability during that time of the year.

5 Conclusion

Despite climate warming, aperiodic deep winter turnover still occurs in Lake Zurich. Deep-water warming can facilitate deep mixing events, as an increasing heat content of hypolimnetic water allows homogenization of the water column at higher temperatures. Consequently, the strong epilimnetic enrichment by PO_4 that has accumulated in the deep zone during previous periods of incomplete mixing, can promote intense blooms of centric diatoms and cryptophytes. Only a few ciliate species (*Balanion planctonicum*, *Urotricha* spp. <25µm and tintinnids) significantly increased their abundances during the first half of spring 2021 (deep mixing), compared to the adjacent years, whereas others showed only short-term abundance peaks and otherwise similar trends than in 2020/2022. Thus, the total ciliate assemblage showed a surprisingly high resilience in terms of morphotype composition. However, most planktonic ciliate species have been taxonomically described based on microscopy. Current research focuses on the potential cryptic genetic diversity within ciliate morphospecies, and which diagnostic features need to be examined to define it (Rajter et al., 2022; Smith et al., 2022). Therefore, apparent resilience of the composition of ciliate morphotypes may mask genotypic shifts within distinct morphotypes. While knowledge about the cryptic diversity of planktonic ciliate species is still in its infancy, new methodological tools are emerging (Dirren-Pitsch et al., 2022), that will open new perspectives on studying this topic.

Data availability statement

The original contributions presented in the study are included in the article/Supplementary Material. Further inquiries can be directed to the corresponding author.

Author contributions

MS-S: Writing – review & editing, Writing – original draft, Visualization, Validation, Supervision, Methodology, Investigation, Formal analysis, Data curation, Conceptualization. AW: Writing – review & editing, Visualization, Validation, Methodology, Formal analysis. GD-P: Writing – review & editing, Visualization, Validation, Supervision, Methodology, Investigation, Formal analysis. RN: Writing – review & editing, Methodology, Investigation, Data curation. BB: Writing – review & editing, Methodology, Investigation, Data curation. OK: Writing – review & editing, Data curation. JP: Writing – review & editing, Supervision, Resources. TP: Writing – review & editing, Validation, Supervision, Resources, Project administration, Methodology, Investigation, Funding acquisition, Formal analysis, Data curation, Conceptualization.

Funding

The author(s) declare financial support was received for the research, authorship, and/or publication of this article. This study was supported by the Swiss National Science Foundation grants 31003A_182489 and 31003A_182336.

Acknowledgments

We thank E. Loher and D. Marty for all the help during the intensive sampling campaign. We thank the Water Police Zurich for providing meteorological data and the federal government (BAFU) for discharge values of Lake Zurich.

Conflict of interest

The authors declare that the research was conducted in the absence of any commercial or financial relationships that could be construed as a potential conflict of interest.

Publisher's note

Supplementary material

The Supplementary Material for this article can be found online at: https://www.frontiersin.org/articles/10.3389/frpro.2024.1428985/full#supplementary-material

References

Agatha, S., Laval-Peuto, M., and Simon, P. (2012). "The tintinnid lorica," in *The biology and ecology of tintinnid ciliates*. Eds. J. R. Dolan, D. J. S. Montagnes, S. Agatha, D. W. Coats and D. K. Stoecker (Wiley-Blackwell, United State), 17–41.

Beutler, M., Wiltshire, K. H., Meyer, B., Moldaenke, C., Lüring, C., Meyerhöfer, M., et al. (2002). A fluorometric method for the differentiation of algal populations *in vivo* and in *situ*. *Photosynth. Res.* 72, 39–53. doi: 10.1023/A:1016026607048

Bleiker, W., and Schanz, F. (1989). Influence of environmental factors on the phytoplankton spring bloom in Lake Zürich. *Aquat. Sci.* 51, 47–58. doi: 10.1007/BF00877780

Blom, J. F., Bister, B., Bischoff, D., Nicholson, G., Jung, G., Süssmuth, R. D., et al. (2003). Oscillapeptin J, a new grazer toxin of the freshwater cyanobacterium *Planktothrix rubescens*. *J. Nat. Prod.* 66, 431–434. doi: 10.1021/np020397f

Børsheim, K. Y., and Bratbak, G. (1987). Cell volume to cell carbon conversion factors for a bacterivorous *Monas* sp. enriched from seawater. *Mar. Ecol. Prog. Ser.* 36, 171–175. doi: 10.3354/meps036171

Bossard, P., Gammeter, S., Lehmann, C., Schanz, F., Bachofen, R., Bürgi, H.-R., et al (2001). Limnological description of the Lakes Zurich, Lucerne, and Cadagno. *Aquat. Sci.* 63, 225–249. doi: 1007/PL000013533

Desgué-Itier, O., Melo Vieira Soares, L., Anneville, O., Bouffard, D., Chanudet, V., Danis, P. A., et al. (2023). Past and future climate change effects on the thermal regime and oxygen solubility of four peri-alpine lakes. *Hydrol. Earth Syst. Sci.* 27, 837–859. doi: 10.5194/hess-27-837-2023

Dirren-Pitsch, G., Bühler, D., Salcher, M. M., Bassin, B., Le Moigne, A., Schuler, M., et al. (2022). FISHing for ciliates: Catalyzed reporter deposition fluorescence in *situ* hybridization for the detection of planktonic freshwater ciliates. *Front. Microbiol.* 13. doi: 10.3389/fmicb.2022.1070232

Doda, T., Ramón, C. L., Ulloa, H. N., Wüest, A., and Bouffard, D. (2022). Seasonality of density currents induced by differential cooling. *Hydrol. Earth Syst. Sci.* 26, 331–353. doi: 10.5194/hess-26-331-2022

Doda, T., Ulloa, H. N., Ramón, C. L., Wüest, A., and Bouffard, D. (2023). Penetrative convection modifies the dynamics of downslope gravity currents. *Geophys. Res. Lett.* 50, e2022GL100633. doi: 10.1029/2022GL100633

Dokulil, M. T. (2014). Impact of climate warming on European inland waters. *Inl. Waters* 4, 27–40. doi: 10.5268/IW-4.1.705

Dokulil, M. T., de Eyto, E., Maberly, S. C., May, L., Weyhenmeyer, G. A., and Woolway, R. I. (2021). Increasing maximum lake surface temperature under climate change. *Clim. Change* 165, 56. doi: 10.1007/s10584-021-03085-1

Eckert, E. M., Baumgartner, M., Huber, I. M., and Pernthaler, J. (2013). Grazing resistant freshwater bacteria profit from chitin and cell-wall-derived organic carbon. *Environ. Microbiol.* 15, 2019–2030. doi: 10.1111/1462-2920.12083

Eckert, E. M., Salcher, M. M., Posch, T., Eugster, B., and Pernthaler, J. (2012). Rapid successions affect microbial N-acetyl-glucosamine uptake patterns during a lacustrine spring phytoplankton bloom. *Environ. Microbiol.* 14, 794–806. doi: 10.1111/j.1462-2920.2011.02639.x

Egge, J. K., and Aksnes, D. L. (1992). Silicate as regulating nutrient in phytoplankton competition. *Mar. Ecol. Prog. Ser.* 83, 281–289. doi: 10.3354/meps083281

Einsele, (1936). Über die Beziehungen des Eisenkreislaufs zum Phosphatkreislauf im eutrophen See. *Arch. für Hydrobiol.* 29, 664–686.

Esteban, G. F., and Fenchel, T. M. (2020). *Ecology of protozoa. 2nd ed* (Berlin: Springer Verlag). doi: 10.1007/978-3-030-59979-9

Fenchel, T. (1987). *The biology of free-living phagotrophic protists* (Berlin: Springer Verlag). doi: 10.1007/978-3-030-59979-9

Foissner, W., Berger, H., Blatterer, H., and Kohmann, F. (1995). Taxonomische und ökologische Revision der Ciliaten des Saprobiensystems. Band IV: Gymnostomatea, Loxodes, Suctoria. *Heft 1/95* (Munich: Informationsberichte des Bayerischen Landesamtes für Wasserwirtschaft).

Foissner, W., Berger, H., and Kohmann, F. (1994). Taxonomische und ökologische Revision der Ciliaten des Saprobiensystems – Band III: Hymenostomata, Prostomatida, Nassulida. *Heft 1/94* (Munich: Informationsberichte des Bayerischen Landesamtes für Wasserwirtschaft).

Foissner, W., Berger, H., and Schaumburg, J. (1999). *Identification and ecology of limnetic plankton ciliates. Heft 3/99* (Munich: Informationsberichte des Bayerischen Landesamtes für Wasserwirtschaft).

Foissner, W., Blatterer, H., Berger, H., and Kohmann, F. (1992). Taxonomische und ökologische Revision der Ciliaten des Saprobiensystems. Band II: Peritrichia, Heterotrichida, Odontostomatida. *Heft 5/92* (Munich: Informationsberichte des Bayerischen Landesamtes für Wasserwirtschaft).

Foissner, W., Blatterer, H., and Kohmann, F. (1991). Taxonomische und ökologische Revision der Ciliaten des Saprobiensystems – Band I: Cryptophorida, Oligotrichida, Hypotrichia, Colpodea. *Heft 1/91* (Munich: Informationsberichte des Bayerischen Landesamtes für Wasserwirtschaft).

Gao, F., Warren, A., Zhang, Q., Gong, J., Miao, M., Sun, P., et al. (2016). The all-data-based evolutionary hypothesis of ciliated protists with a revised classification of the phylum Ciliophora (Eukaryota, Alveolata). *Sci. Rep.* 6, 24874. doi: 10.1038/srep24874

Gilbert, J. J. (1994). Jumping behavior in the oligotrich ciliates *Strobilidium velox* and *Halteria grandinella*, and its significance as a defense against rotifer predators. *Microb. Ecol.* 27, 189–200. doi: 10.1007/BF00165817

Gilbert, J. J. (2022). Food niches of planktonic rotifers: Diversification and implications. *Limnol. Oceanogr.* 67, 2218–2251. doi: 10.1002/lno.12199

Hofmann, H., and Peeters, F. (2013). *In-situ* optical and acoustical measurements of the buoyant cyanobacterium *P. rubescens*: Spatial and temporal distribution patterns. *PloS One* 8, e80913. doi: 10.1371/journal.pone.0080913

Holzner, C. P., Aeschbach-Hertig, W., Simona, M., Veronesi, M., Imboden, D. M., and Kipfer, R. (2009). Exceptional mixing events in meromictic Lake Lugano (Switzerland/Italy), studied using environmental tracers. *Limnol. Oceanogr.* 54, 1113–1124. doi: 10.4319/lo.2009.54.4.1113

Huisman, J., Sharples, J., Stroom, J. M., Visser, P. M., Kardinaal, W. E. A., Verspagen, J. M. H., et al. (2004). Changes in turbulent mixing shift competition for light between phytoplankton species. *Ecology* 85, 2960–2970. doi: 10.1890/03-0763

Knapp, D., Fernández Castro, B., Marty, D., Loher, E., Köster, O., Wüest, A., et al. (2021). The red harmful plague in times of climate change: Blooms of the cyanobacterium *Planktothrix rubescens* triggered by stratification dynamics and irradiance. *Front. Microbiol.* 12. doi: 10.3389/fmicb.2021.70591

Kurmayer, R., Deng, L., and Entfellner, E. (2016). Role of toxic and bioactive secondary metabolites in colonization and bloom formation by filamentous cyanobacteria Planktothrix. *Harmful Algae* 54, 69–86. doi: 10.1016/j.hal.2016.01.004

Leboulanger, C., Dorigo, U., Jacquet, S., Le Berre, B., Paolini, G., and Humbert, J. F. (2002). Application of a submersible spectrofluorometer for rapid monitoring of freshwater cyanobacterial blooms: a case study. *Aquat. Microb. Ecol.* 30, 83–89. doi: 10.3354/ame030083

Lepori, F., Bartosiewicz, M., Simona, M., and Veronesi, M. (2018). Effects of winter weather and mixing regime on the restoration of a deep perialpine lake (Lake Lugano, Switzerland and Italy). *Hydrobiologia* 824, 229–242. doi: 10.1007/s10750-018-3575-2

Lynn, D. H. (2008). *The ciliated protozoa. Characterization, classification, and guide to the literature. 3rd ed* (Dordrecht: Springer Netherlands). doi: 10.1007/978-1-4020-8239-9

Macek, M., Šimek, K., Pernthaler, J., Vyhnálek, V., and Psenner, R. (1996). Growth rates of dominant planktonic ciliates in two freshwater bodies of different trophic degree. *J. Plankton Res.* 18, 463–481. doi: 10.1093/plankt/18.4.463

Menden-Deuer, S., and Lessard, E. J. (2000). Carbon to volume relationships for dinoflagellates, diatoms, and other protist plankton. *Limnol. Oceanogr.* 45, 569–579. doi: 10.4319/lo.2000.45.3.0569

MeteoSwiss (2021). *Klimabulletin sommer 2021* (Zürich). Available online at: https://www.meteoschweiz.admin.ch/service-und-publikationen/publikationen/berichte-und-bulletins/2021/klimabulletin-sommer-2021.html (Accessed January 19, 2024).

Mindl, B., Sonntag, B., Pernthaler, J., Vrba, J., Psenner, R., and Posch, T. (2005). Effects of phosphorus loading on interactions of algae and bacteria: Reinvestigation of the "phytoplankton-bacteria paradox" in a continuous cultivation system. *Aquat. Microb. Ecol.* 38, 203–213. doi: 10.3354/ame038203

Montagnes, D. J. S., Berges, J. A., Harrison, P. J., and Taylor, F. J. R. (1994). Estimating carbon, nitrogen, protein, and chlorophyll a from volume in marine phytoplankton. *Limnol. Oceanogr.* 39, 1044–1060. doi: 10.4319/lo.1994.39.5.1044

Mortimer, C. H. (1942). The exchange of dissolved substances between mud and water in lakes. *J. Ecol.* 29, 147–201. doi: 10.2307/2256691

Müller, H., and Geller, W. (1993). Maximum growth rates of aquatic ciliated protozoa: the dependence on body size and temperature reconsidered. *Arch. für Hydrobiol.* 126, 315–327. doi: 10.1127/archiv-hydrobiol/126/1993/315

Müller, H., and Schlegel, A. (1999). Responses of three freshwater planktonic ciliates with different feeding modes to cryptophyte and diatom prey. *Aquat. Microb. Ecol.* 17, 49–60. doi: 10.3354/ame017049

O'Reilly, C. M., Alin, S. R., Piisnier, P. D., Cohen, A. S., and McKee, B. A. (2003). Climate change decreases aquatic ecosystem productivity of Lake Tanganyika, Africa. *Nature* 424, 766–768. doi: 10.1038/nature01833

O'Reilly, R. R.J., Schneider, P., Lenters, J. D., Mcintyre, P. B., and Kraemer, B. M. (2015). Rapid and highly variable warming of lake surface waters around the globe. *Geophys. Res. Lett.* 42, 10773–10781. doi: 10.1002/2015GL066235

Örn, C. G., Schanz, F., and Thomas, E. A. (1981). An empirical model relating wind action and hypolimnetic oxygenation during vernal circulation in Lake Zurich from 1950–1979. *Verhandlungen Des. Int. Verein Limnol.* 21, 109–114. doi: 10.1080/03680770.1980.11896965

Pauli, H. R. (1989). A new method to estimate individual dry weights of rotifers. *Hydrobiologia* 186, 355–361. doi: 10.1007/BF00048932

Peeters, F., Livingstone, D. M., Goudsmit, G. H., Kipfer, R., and Forster, R. (2002). Modeling 50 years of historical temperature profiles in a large central European lake. *Limnol. Oceanogr.* 47, 186–197. doi: 10.4319/lo.2002.47.1.0186

Pfister, G., Sonntag, B., and Posch, T. (1999). Comparison of a direct live count and an improved quantitative protargol stain (QPS) in determining abundance and cell volumes of pelagic freshwater protozoa. *Aquat. Microb. Ecol.* 18, 95–103. doi: 10.3354/ame018095

Pitsch, G. (2015). Morphological and molecular based analyses of planktonic ciliates in Lake Zurich. University of Zurich, Zurich (CH).

Pitsch, G., Bruni, E. P., Forster, D., Qu, Z., Sonntag, B., Stoeck, T., et al. (2019). Seasonality of planktonic freshwater ciliates: Are analyses based on V9 regions of the 18S rRNA gene correlated with morphospecies counts? *Front. Microbiol.* 10. doi: 10.3389/fmicb.2019.00248

Posch, T., Eugster, B., Pomati, F., Pernthaler, J., Pitsch, G., and Eckert, E. M. (2015). Network of interactions between ciliates and phytoplankton during spring. *Front. Microbiol.* 6. doi: 10.3389/fmicb.2015.01289

Posch, T., Franzoi, J., Prader, M., and Salcher, M. M. (2009). New image analysis tool to study biomass and morphotypes of three major bacterioplankton groups in an alpine lake. *Aquat. Microb. Ecol.* 54, 113–126. doi: 10.3354/ame01269

Posch, T., Köster, O., Salcher, M. M., and Pernthaler, J. (2012). Harmful filamentous cyanobacteria favored by reduced water turnover with lake warming. *Nat. Clim. Change* 2, 809–813. doi: 10.1038/nclimate1581

Posch, T., Pitsch, G., and Bruni, E. P. (2022). "Protists: ciliates," in *Encyclopedia of inland waters* (Elsevier, Oxford), 639–649. doi: 10.1016/B978-0-12-819166-8.00001-3

Porter, K. G., and Feig, Y. S. (1980). The use of DAPI for identifying and counting aquatic microflora. *Limnol. Oceanogr.* 25, 943–948. doi: 10.4319/lo.1980.25.5.0943

Rajter, Ľ., Lu, B., Rassoshanska, E., and Dunthorn, M. (2022). Future prospects for investigating ciliate biodiversity. *Acta Protozool.* 61, 35–46. doi: 10.4467/16890027AP.22.005.16236

Råman Vinnå, L., Medhaug, I., Schmid, M., and Bouffard, D. (2021). The vulnerability of lakes to climate change along an altitudinal gradient. *Commun. Earth Environ.* 2, 35. doi: 10.1038/s43247-021-00106-w

Reynolds, C. S. (2006). *The ecology of phytoplankton* (Cambridge: Cambridge University Press). doi: 10.1017/CBO9780511542145

Salmaso, N., Boscaini, A., Capelli, C., and Cerasino, L. (2018). Ongoing ecological shifts in a large lake are driven by climate change and eutrophication: evidences from a three-decade study in Lake Garda. *Hydrobiologia* 824, 177–195. doi: 10.1007/s10750-017-3402-1

Sanders, R., and Wickham, S. A. (1993). Planktonic protozoa and metazoa: Predation, food quality and population control. *Mar. Microb. Food Webs* 7, 197–223.

Santoferrara, L. F., Grattepanche, J.-D., Katz, L. A., and McManus, G. B. (2014). Pyrosequencing for assessing diversity of eukaryotic microbes: analysis of data on marine planktonic ciliates and comparison with traditional methods. *Environ. Microbiol.* 16, 2752–2763. doi: 10.1111/1462-2920.12380

Schanz, F. (1986). Depth distribution of phytoplankton and associated spectral changes in downward irradiance in Lake Züric/81). *Hydrobiologia* 134, 183–192. doi: 10.1007/BF00006740

Schmid, M., and Köster, O. (2016). Excess warming of a Central European lake driven by solar brightening. *Water Resour. Res.* 52, 8103–8116. doi: 10.1002/2016WR018651

Schneider, P., and Hook, S. (2010). Space observations of inland water bodies show rapid surface warming since 1985. *J. Geophys. Res. Lett.* 37, L22405. doi: 10.1029/2010GL045059

Schuler, M. (2020). *In situ* versus artificial water turnover during spring : A comparison of microbial food web structures. University of Zurich, Zurich (CH).

Schwefel, R., Gaudard, A., Wüest, A., and Bouffard, D. (2016). Effects of climate change on deepwater oxygen and winter mixing in a deep lake (Lake Geneva): Comparing observational findings and modeling. *Water Resour. Res.* 52, 8811–8826. doi: 10.1002/2016WR019194

Schwefel, R., Müller, B., Boisgontier, H., and Wüest, A. (2019). Global warming affects nutrient upwelling in deep lakes. *Aquat. Sci.* 81, 50. doi: 10.1007/s00027-019-0637-0

Shimoda, Y., Azim, M. E., Perhar, G., Ramin, M., Kenney, M. A., Sadraddini, S., et al. (2011). Our current understanding of lake ecosystem response to climate change: What have we really learned from the north temperate deep lakes? *J. Great Lakes Res.* 37, 173–193. doi: 10.1016/j.jglr.2010.10.004

Šimek, K., Grujčić, V., Nedoma, J., Jezberová, J., Šorf, M., Matoušů, A., et al. (2019). Microbial food webs in hypertrophic fishponds: Omnivorous ciliate taxa are major protistan bacterivores. *Limnol. Oceanogr.* 64, 2295–2309. doi: 10.1002/lno.11260

Skibbe, O. (1994). An improved quantitative protargol stain for ciliates and other planktonic protists. *Arch. für Hydrobiol.* 130, 339–347. doi: 10.1127/archiv-hydrobiol/130/1994/339

Skogstad, A., Granskog, L., and Klaveness, D. (1987). Growth of freshwater ciliates offered planktonic algae as food. *J. Plankton Res.* 9, 503–512. doi: 10.1093/plankt/9.3.503

Smetacek, V. S. (1985). Role of sinking in diatom life-history cycles: ecological, evolutionary and geological significance. *Mar. Biol.* 84, 239–251. doi: 10.1007/BF00392493

Smith, S. A., Santoferrara, L. F., Katz, L. A., and McManus, G. B. (2022). Genome architecture used to supplement species delineation in two cryptic marine ciliates. *Mol. Ecol. Resour.* 22, 2880–2896. doi: 10.1111/1755-0998.13664

Sommer, U., Adrian, R., De Senerpont Domis, L., Elser, J. J., Gaedke, U., Ibelings, B., et al. (2012). Beyond the plankton ecology group (PEG) model: Mechanisms driving plankton succession. *Annu. Rev. Ecol. Evol. Syst.* 43, 429–448. doi: 10.1146/annurev-ecolsys-110411-160251

Sommer, U., Gliwicz, Z. M., Lampert, W. I., and Duncan, A. (1986). The PEG-model of seasonal succession of planktonic events in fresh waters. *Arch. fur Hydrobiol.* 106, 433–471. doi: 10.1127/archiv-hydrobiol/106/1986/433

Sonntag, B., Posch, T., Klammer, S., Teubner, K., and Psenner, R. (2006). Phagotrophic ciliates and flagellates in an oligotrophic, deep, alpine lake: Contrasting variability with seasons and depths. *Aquat. Microb. Ecol.* 43, 193–207. doi: 10.3354/ame043193

Telesh, I. V., Rahkola, M., and Viljanen, M. (1998). Carbon content of some freshwater rotifers. *Hydrobiologia* 388, 355–360. doi: 10.1007/978-94-011-4782-8_47

Tirok, K., and Gaedke, U. (2007). Regulation of planktonic ciliate dynamics and functional composition during spring in Lake Constance. *Aquat. Microb. Ecol.* 49, 87–100. doi: 10.3354/ame01127

Toffolon, M., Piccolroaz, S., Majone, B., Soja, A. M., Peeters, F., Schmid, M., et al. (2014). Prediction of surface temperature in lakes with different morphology using air temperature. *Limnol. Oceanogr.* 59, 2185–2202. doi: 10.4319/lo.2014.59.6.2185

Urabe, J., Gurung, T. B., Yoshida, T., Sekino, T., Nakanishi, M., Maruo, M., et al. (2000). Diel changes in phagotrophy by Cryptomonas in Lake Biwa. *Limnol. Oceanogr.* 45, 1558–1563. doi: 10.4319/lo.2000.45.7.1558

Utermöhl, H. (1958). Zur Vervollkommnung der quantitativen Phytoplankton-Methodik. *Mitt. Int. Verein. Theor. Angew. Limnol.* 9, 1–38.

Walsby, A. E., Avery, A., and Schanz, F. (1998). The critical pressures of gas vesicles in *Planktothrix rubescens* in relation to the depth of winter mixing in Lake Zurich, Switzerland. *J. Plankton Res.* 20, 1357–1375. doi: 10.1093/plankt/20.7.1357

Weisse, T. (2017). Functional diversity of aquatic ciliates. *Eur. J. Protistol.* 61, 331–358. doi: 10.1016/j.ejop.2017.04.001

Weisse, T., and Frahm, A. (2002). Direct and indirect impact of two common rotifer species (*Keratella* spp.) on two abundant ciliate species (*Urotricha furcata*, *Balanion planctonicum*). *Freshw. Biol.* 47, 53–64. doi: 10.1046/j.1365-2427.2002.00780.x

Weisse, T., Karstens, N., Meyer, V. C. L., Janke, L., Lettner, S., and Teichgräber, K. (2001). Niche separation in common prostome freshwater ciliates: The effect of food and temperature. *Aquat. Microb. Ecol.* 26, 167–179. doi: 10.3354/ame026167

Woolway, R. I., Kraemer, B. M., Lenters, J. D., Merchant, C. J., O'Reilly, C. M., and Sharma, S. (2020). Global lake responses to climate change. *Nat. Rev. Earth Environ.* 1, 388–403. doi: 10.1038/s43017-020-0067-5

Woolway, R. I., and Merchant, C. J. (2019). Worldwide alteration of lake mixing regimes in response to climate change. *Nat. Geosci.* 12, 271–276. doi: 10.1038/s41561-019-0322-x

Yankova, Y., Neuenschwander, S., Köster, O., and Posch, T. (2017). Abrupt stop of deep water turnover with lake warming: Drastic consequences for algal primary producers. *Sci. Rep.* 7, 13770. doi: 10.1038/s41598-017-13159-9

Yankova, Y., Villiger, J., Pernthaler, J., Schanz, F., and Posch, T. (2016). Prolongation, deepening and warming of the metalimnion change habitat conditions of the harmful filamentous cyanobacterium *Planktothrix rubescens* in a prealpine lake. *Hydrobiologia* 776, 125–138. doi: 10.1007/s10750-016-2745-3

Yoo, Y., Seong, K. A., Jeong, H. J., Yih, W., Rho, J.-R., Nam, S. W., et al. (2017). Mixotrophy in the marine red-tide cryptophyte *Teleaulax amphioxeia* and ingestion and grazing impact of cryptophytes on natural populations of bacteria in Korean coastal waters. *Harmful Algae* 68, 105–117. doi: 10.1016/j.hal.2017.07.012

Zeder, M., Peter, S., Shabarova, T., and Pernthaler, J. (2009). A small population of planktonic Flavobacteria with disproportionally high growth during the spring phytoplankton bloom in a prealpine lake. *Environ. Microbiol.* 11, 2676–2686. doi: 10.1111/j.1462-2920.2009.01994.x